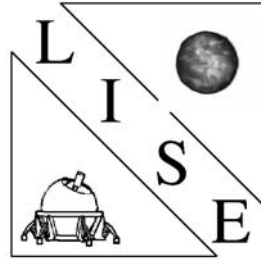# OWL INSTRUMENT CONCEPT STUDY

HYPERTELESCOPE CAMERA FOR INITIAL OBSERVING WITH THE UNFILLED PRIMARY MOSAIC

Olivier Lardière [1], Virginie Borkowski [1] and Antoine Labeyrie [1]

[1] LISE - Collège de France, Observatoire de Haute Provence, 04870 St Michel l'Observatoire.

OWL-CSR-ESO-00000-0167 — Version 1.0

Date: 11 October 2005

1. Introduction

During the fabrication and installation of the M1 mirror segments, it will be of interest to optimize the filling of the 100m aperture for achieving the best science during these few years. We have studied a densified-pupil mode (see section 2) to improve the sensitivity of OWL during its progressive implementation phase (see Chapter 2.7 in the OWL Concept Design Report) . Sections 3 trough 7 discuss different filling configurations and their intensification gain. In section 8 we mention a speckle interferometry mode suitable for observing faint objects in the absence of adaptive optics, or of a guide star sufficiently bright to activate it. In section 9, we propose an adaptive fringe sensor unit to cophase all the segments. Finally, in section 10 and 11, we briefly mention the adaptive imaging mode with a densified array and a coronagraphic mode for imaging extra-solar planets.

2. Principle of hypertelescope

As previously described (Labeyrie et al. 1996 and Fig.1), a hypertelescope is a multi-element imaging interferometric array having a densified pupil. It allows direct imaging with high resolution. Indeed, densifying a pupil increases the ratio of the sub-aperture diameters to their spacing. It can be done by bringing closer optically the entrance sub-apertures or by increasing their diameter. It does not degrade the image properties if the geometrical pattern formed by the center of each mirror is preserved. In an image given by a Fizeau interferometer, the light energy is spread across secondary peaks, unlike in an image given by a hypertelescope where almost all the energy is concentrated in the central peak surrounding by very few secondary dispersed peaks.
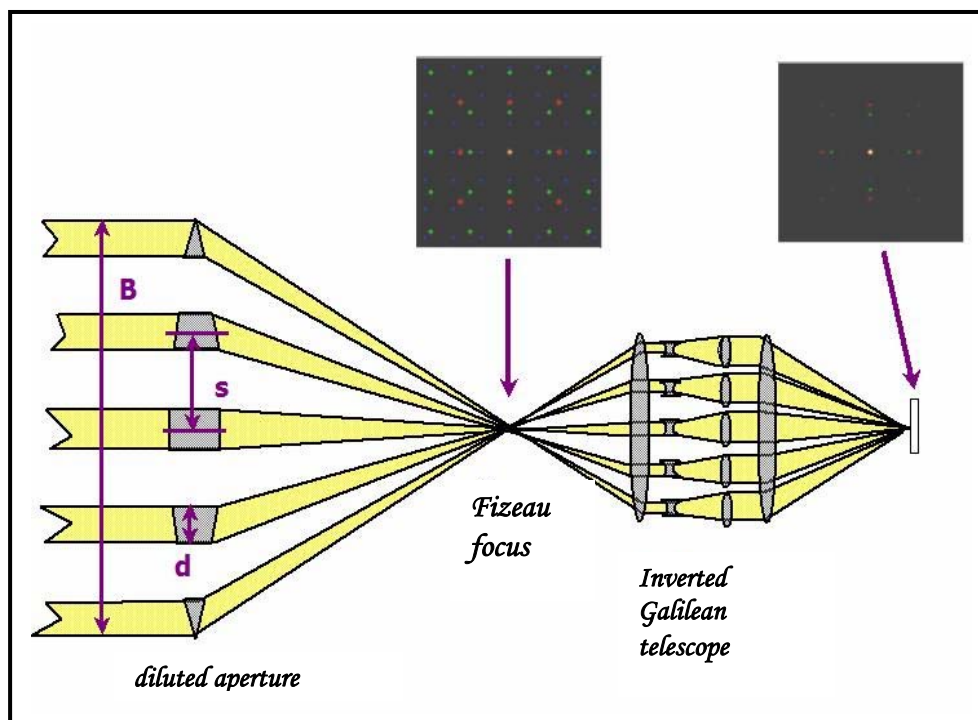

Figure 1: Principle of hypertelescope

3. Pupil filling strategy

The choice of the pupil configuration is a general problem of stellar interferometry. There is a trade-off between field of view (FOV) and the dynamic-range. For the same number of sub-apertures, the largest FOV is provided by a uniform uv-plane filling, while the best dynamic-range is provided by a uniform pupil plane filling. Then the filling strategy depends mainly of on the application: a redundant segment array will be more advantageous for faint compact sources imaging and stellar coronagraphy, while a non-redundant segment array will be more advantageous for imaging complex extended sources.

Moreover, the hypertelescope mode does not generate any field losses if the sub-aperture size is negligible compared to the baselines. In this case the accessible field is only limited by the number of independent simultaneous baselines, whatever the beam combination scheme (Fizeau, densified mode, etc.) (Lardière et. al 2005). Then, in the case of the partially filled OWL, the hypertelescope mode is more interesting if the pupil is made of many regularly spaced isolated segments, rather than few large segments groups.

The ideal entrance pupil for a hypertelescope is a segment array uniformly diluted in both directions, as studied in section 4. This however implies a non-connex entrance pupil, precluding the use of edge-sensors for shaping. This is a very strong constraint for the OWL hypertelescope mode, because a connex shape cannot be densified homogeneously. Indeed, the conventional hypertelescope scheme uses an homogenous and isotropic pupil densification (i.e. the pupil densification factor is the same for all the sub-apertures and isotropic).

To overcome this problem, one can mask the "annoying" segments (the bridges linking the useful segments) and keep only segments regularly spaced. But this solution induces a strong sensitivity loss (see section 5).

To reduce the number of masked segments, one can fill M1 along parallel lines and apply an anisotropic (but homogenous) pupil densification. We lose only one orthogonal branch of segments (see section 6).

In principle, one can densify any pupil shapes with an anisotropic and heterogeneous pupil densification, but the sensitivity gain provided by such a pupil densification will be lower than in the previous cases. Section 7 shows an example with a pupil made of concentric rings and a radial pupil densification.

Note: The following PSF computations are made for circular rather than hexagonal segments, for simplicity. Indeed, the segment shape has little effect in this comparative study. The PSF profile is identical within the diffractive lobe of one segment.

4. Non-connex pupil case

We consider here a non-connex array of segments, uniformly diluted. This is the ideal case for an hypertelescope giving the best sensitivity gain compared to the Fizeau mode. After the first year of segment installation, 254 segments will be available. This can fill one out of every four slots (linearly) to produce a uniform array involving 194 segments. In this case, the densification factor is also 4, then the central peak intensity gain reaches 16 (Figure 2).
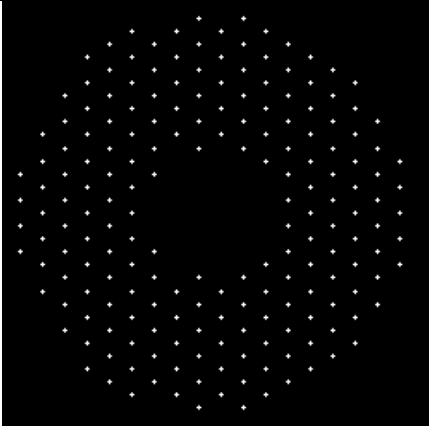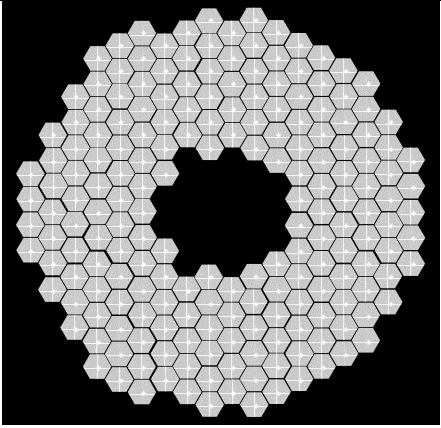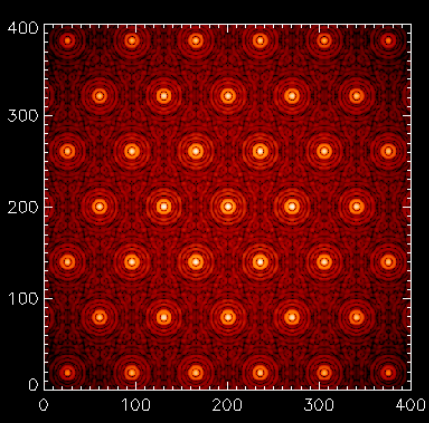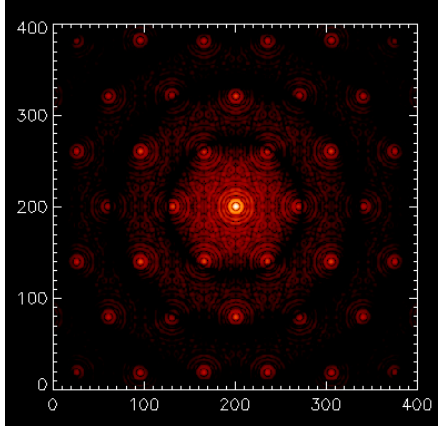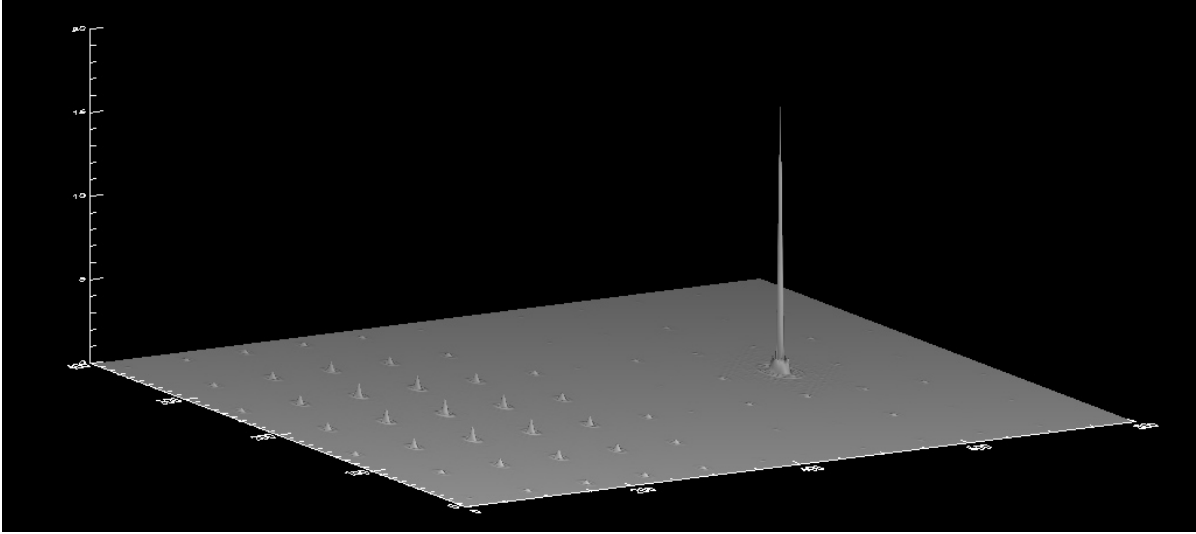
	Fizeau case	Densified pupil case
Exit pupil		
PSF (log scale from 1 to 10^{-6})		
PSFs compared at linear scale		
Max(PSF)	1.00	16.0

Figure 2: Homogenous pupil densification applied on a uniform segment array. Top: aperture and densified pupil; middle: corresponding images of a point source on axis, in log scale; bottom: same in linear scale, showing the intensity gain which reaches 16 with 194 segments.

Unfortunately, this non-connex pupil may be inadequate for OWL, unless a cophasing technique such as "dispersed speckle" could replace the edge sensors. But this would work

only in the presence of a guide star, and would presumably be badly affected by even brief cloud crossings .

5. Connex pupil with homogenous pupil densification

We consider here a contiguous pupil shape exploiting the full resolution of a 100m aperture and containing 246 segments (only 254 segment will be available for the 1st year). It resembles an insect with 6 legs linked by a central ring.

We compare PSFs provided by this full pupil, and by a masked pupil in Fizeau and in the densified-pupil modes. The masking lets 24 segments equally spaced over the 100m-pupil allowing a strong pupil densification ($\gamma_d=10$).

However, as we can see on

Figure 3, the sensitivity gain provided by the densification is mitigated by the loss of collecting surface (surface ratio is 24/246), and also by the degraded u,v coverage decreasing the PSF contrast (the Fizeau PSF is spread across more sidelobes after masking). Moreover, the loss of segments induces a strong reduction of the field accessible to the array, amounting to NxN resells in any imaging mode. Lastly, the contrast gain of the densified-pupil PSF is also negligible compared to the full-pupil PSF, inside the direct imaging field (DIF) (Figure 4)

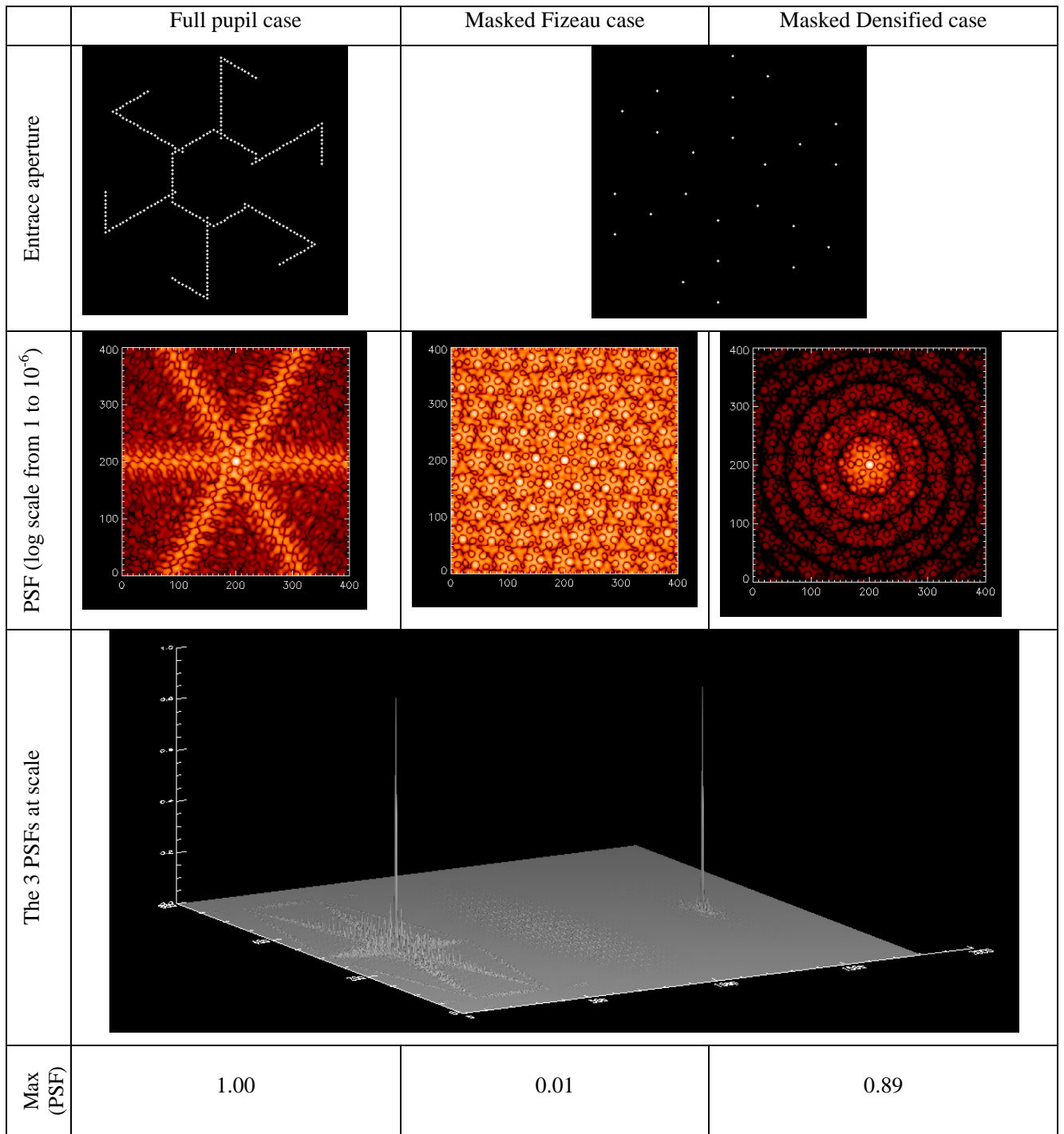|	Full pupil case	Masked Fizeau case	Masked Densified case
Entrace aperture			
PSF (log scale from 1 to 10^{-6})			
The 3 PSFs at scale			
Max (PSF)	1.00	0.01	0.89

Figure 3: Homogenous densification of a connex pupil with some sub-pupils masked. The sensitivity gain provided by the pupil densification is compensated by the loss of collecting surface.
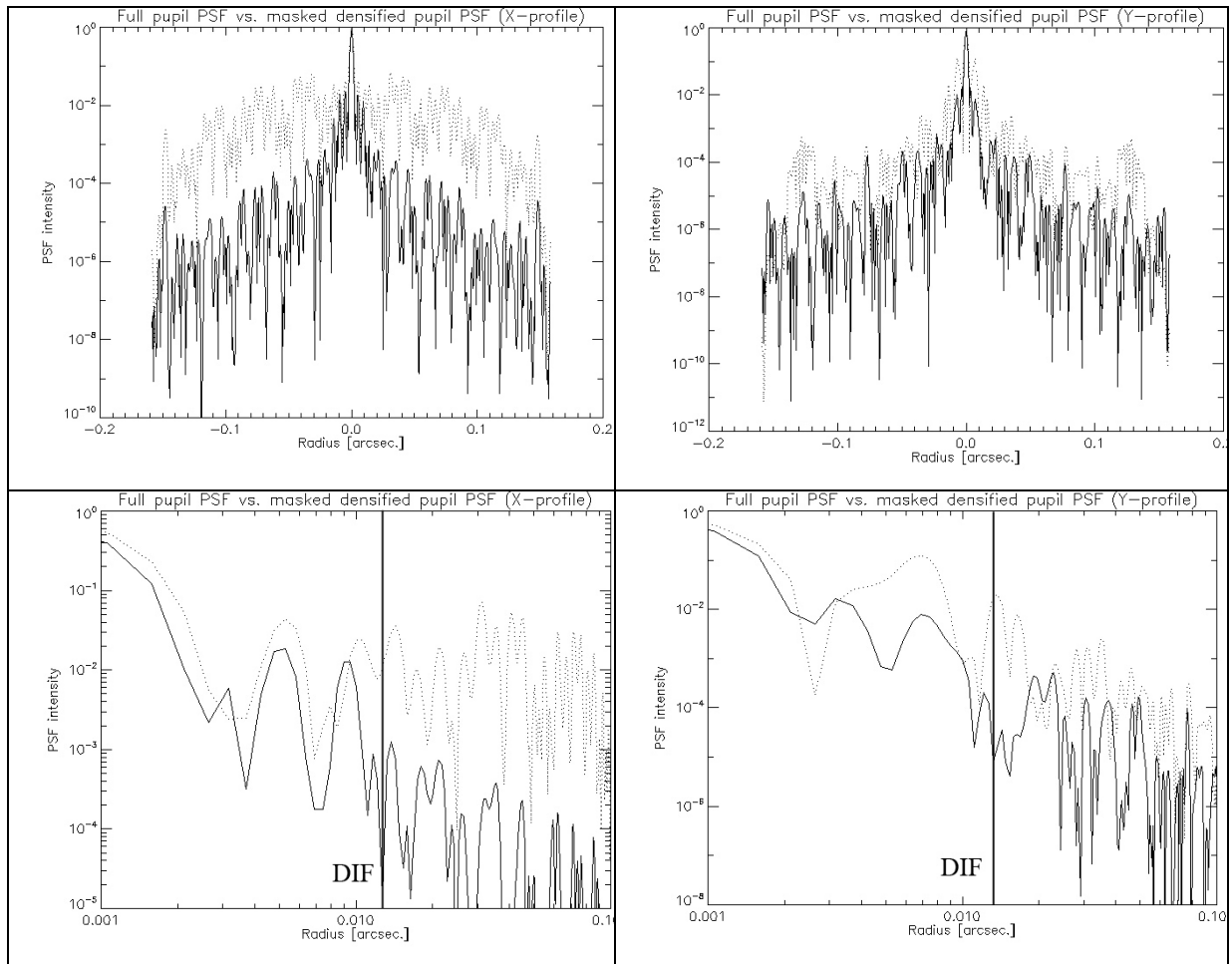
Figure 4: Horizontal (1st column) and vertical (2nd column) cross-sections of the PSF in the full pupil case (dotted curves), and in the masked densified pupil case (solid curve). The first row is a semilog plot, while the second is a loglog plot.

6. Parallel lines and anisotropic pupil densification

6.1 1st implementation year

After the 1st year of implementation, we can fill 5 parallel lines (190 segments) linked by a vertical line (68 segments). The parallel lines are densified orthogonally (γ_d=16) with a non-isotropic pupil densification provided by a pair of cylindrical lens or mirror arrays. Then, only a minor proportion of the segments are lost after masking. The central peak intensity gain reaches 6 after pupil densification.

Such a pupil configuration has an infinite field in one direction (those of the segment lines), and a finite narrow field of view in the perpendicular direction (λ/s if s the line spacing). However, with the field rotation induced by the alt-azimuthal mount of OWL, large complex sources can be imaged by super-synthesis.
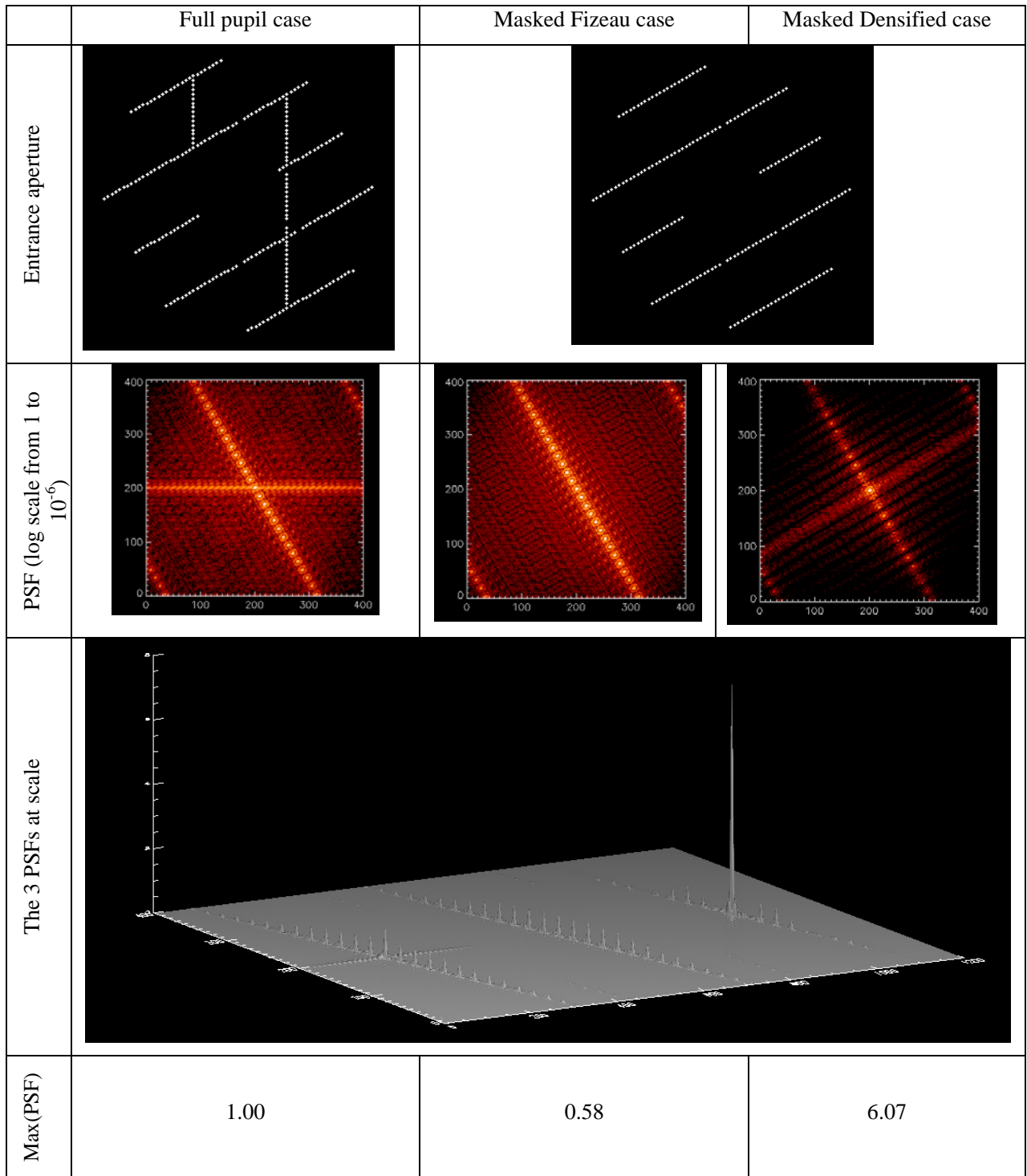
	Full pupil case	Masked Fizeau case	Masked Densified case
Entrance aperture			
PSF (log scale from 1 to 10^{-6})			
The 3 PSFs at scale			
Max(PSF)	1.00	0.58	6.07

Figure 5: Anisotropic densification of a connex pupil having 248 segments (1st year). The intensity gain provided by the pupil densification is 6.07.

6.2 2nd implementation year

During the 2nd year of implementation, 12 parallel lines can be added to the 5 previous lines. This new configuration involves now 791 segments (733 are used for the densification). As the line are more closely spaced, the pupil densification is reduced to 4. The central peak intensity gain is 3.14.
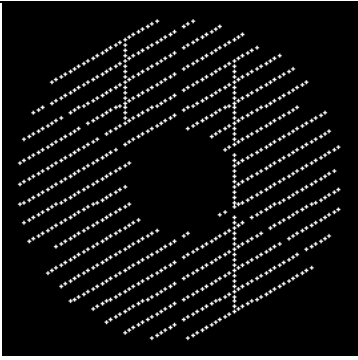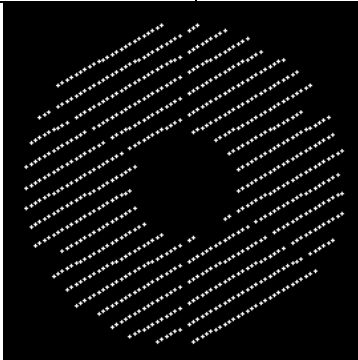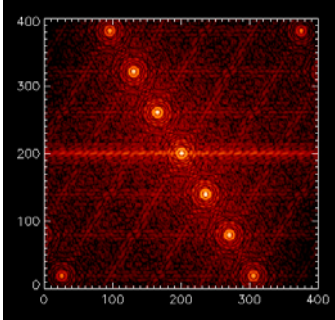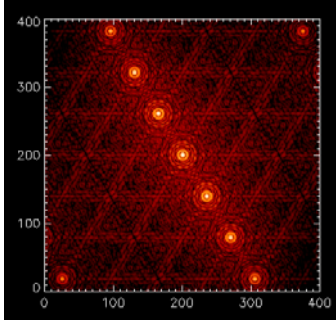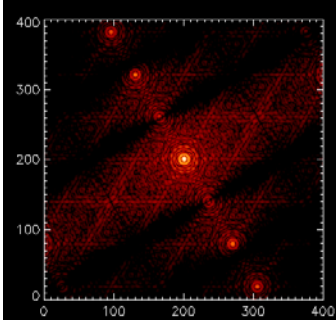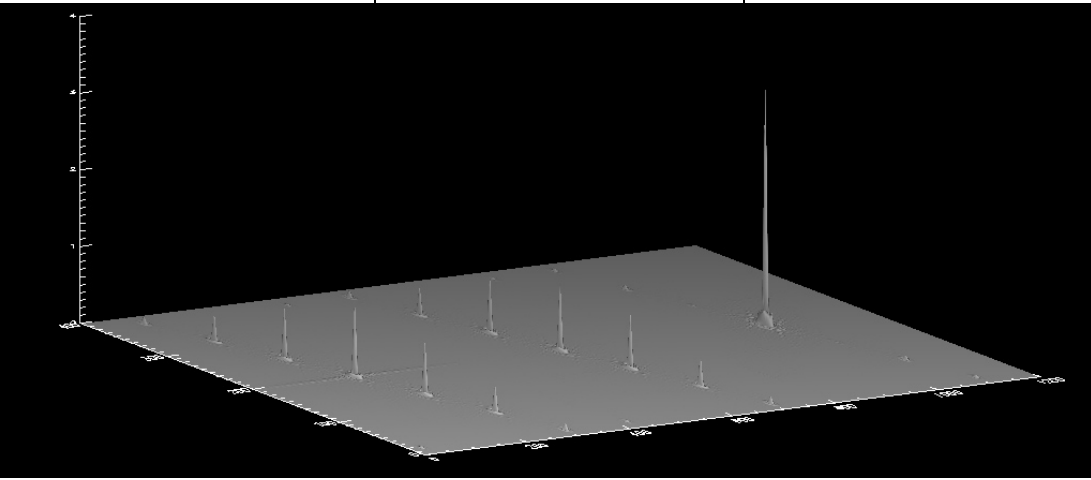
	Full pupil case	Masked Fizeau case	Masked Densified case
Entrance aperture			
PSF (log scale from 1 to 10^{-6})			
The 3 PSFs at scale			
Max (PSF)	1.00	0.88	3.14

Figure 6: Anisotropic densification of a connex pupil involving 791 segments (2nd year). The sensitivity gain provided by the pupil densification is 3.14.

7. Concentric rings and radially densified pupil

The advantage of this configuration is that fewer segments are lost when masking the radial lines connecting the rings. So we do not show here the intermediate Fizeau case after masking (the effect on the PSF of the masking being negligible).

7.1   1st implementation year

With 254 segment, it is possible to fill 2 concentric hexagonal rings linked by a radial branch, with an intensity gain of 5.62.
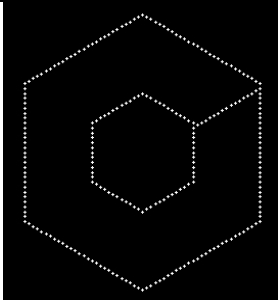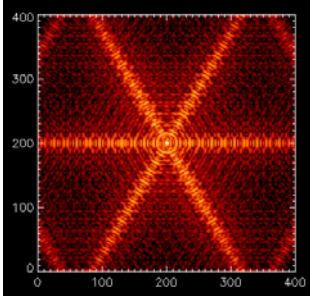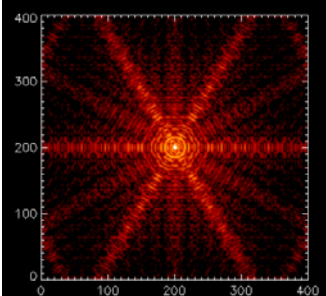
	Fizeau case	Densified case
Entrance aperture		
PSF (log scale from 1 to 10^{-6})		
The 3 PSFs at scale		
Max (PSF)	1.00	5.62

Figure 7: Radial densification of a connex pupil having two concentric rings with 254 segments (1st year). The intensity gain is 5.62.

7.2   2<u>nd</u> implementation year

In the 2nd year it is possible to fill 6 concentric rings., with 775 segments (Figure 8) . The sensitivity gain provided by the pupil densification is 2.26.

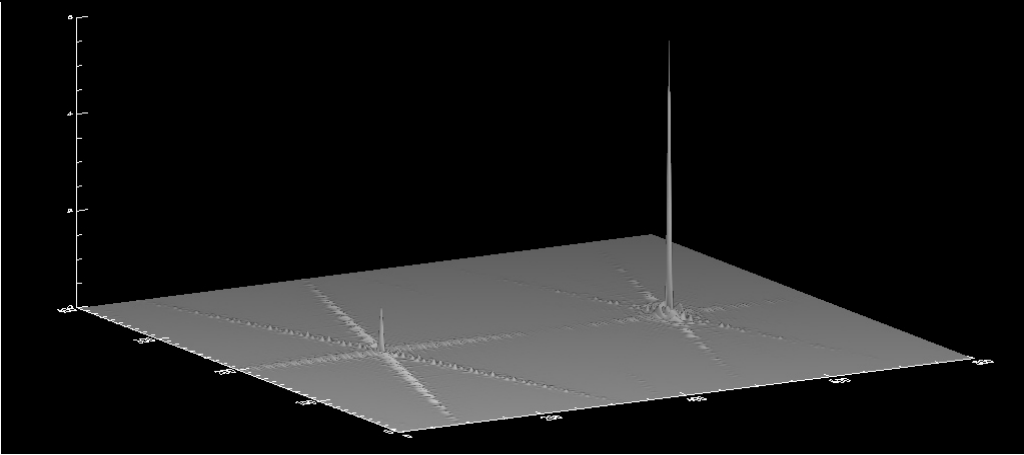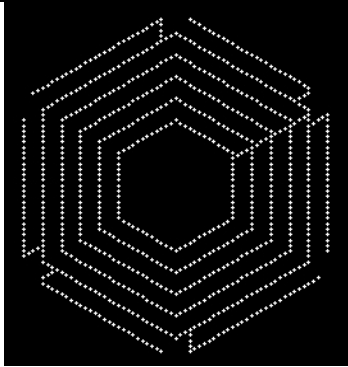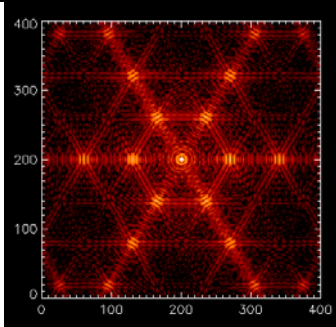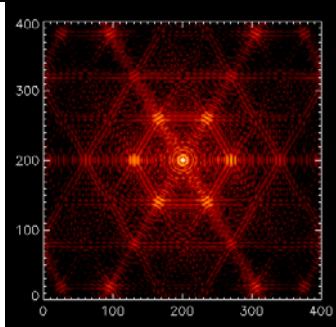|	Fizeau case	Densified case
Entrance aperture		
PSF (log scale from 1 to 10^{-6})		
The 3 PSFs at scale		
Max (PSF)	1.00	2.26

Figure 8: Radial densification of a connex pupil having 6 concentric rings., with 775 segments (2nd year). The sensitivity gain provided by the pupil densification is 2.26.

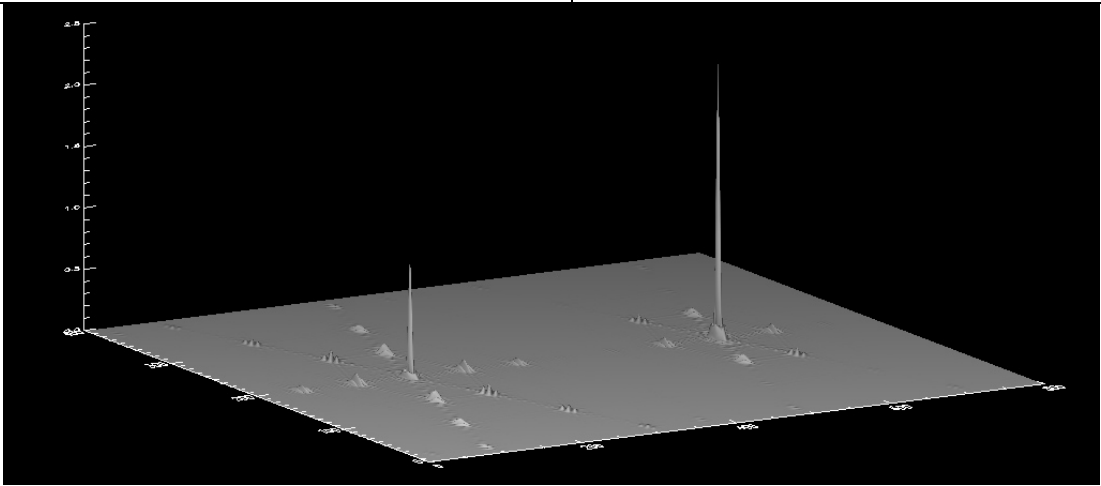## 8. Speckle interferometry with a partially filled aperture

Adaptive optics would be highly desirable also with a partially filled aperture, but requires novel piston sensing methods, such as "Dispersed Speckles", since Shack-Hartmann and curvature sensing cannot deal with diluted apertures. If cophasing system and adaptive optics are not yet available at this stage, or if the field observed contains no guide star which is bright enough, then it can be of interest to do speckle interferometry or speckle masking. These methods work with non-densified and with densified pupils (Figure 9). The dynamic range can be greatly improved if the aperture is non-redundant, to the point where Pegasids 10^4 times fainter than their parent star may become detectable, without adaptive optics , if separated by the 100m baselines. In the northern hemisphere, the planetary companions of 51 Peg and Tau Boo fill this condition and should thus become detectable in red light with an initial OWL having only tens of segments and no cophasing system or adaptive optics.
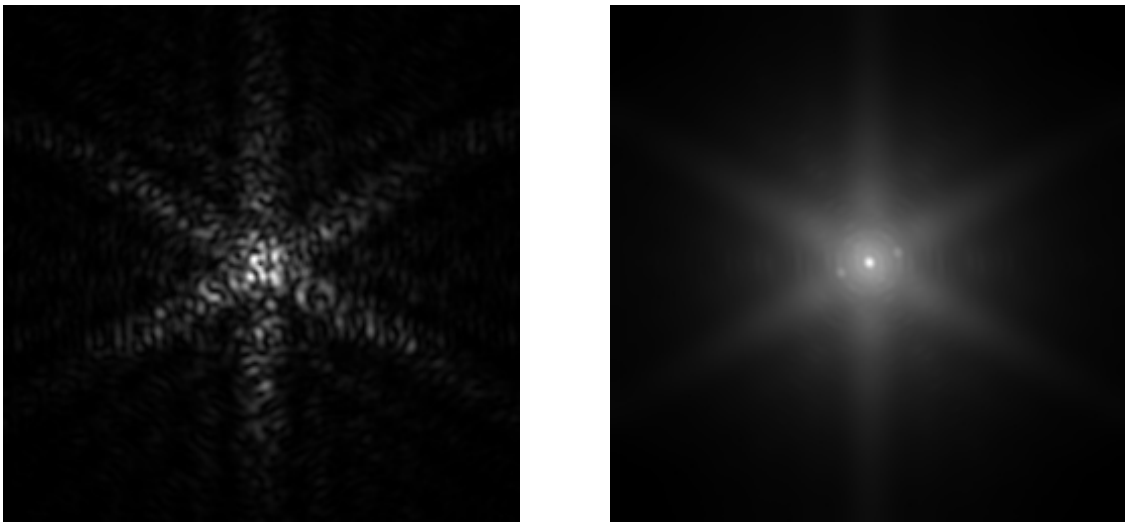

Figure 9: Left: snapshot speckle image of a binary star obtained with a partially filled OWL (2 concentric rings, see 0). Right: autocorrelation of the binary star reconstructed by speckle interferometry from a stack of 350 snapshot images (sep.=8mas, flux ratio=0.5, λ=1µm, r_0=12cm, t_0=6ms).

9. Piston sensing by the "Dispersed Speckles" method

After the speckle interferometry, the next step is long-exposure imaging. With a diluted or a partially filled aperture, long-exposure imaging becomes possible as soon as the segments are cophased, even without adaptive optics inside each segment. Indeed, the correction of the segment piston will froze the interference pattern (i.e. the high-resolution central peak of the PSF), while the residual phase error inside each segment will only affect the envelope shape.

We propose here a cophasing technique, called "dispersed speckles" method, which can directly measure piston errors, in the sub-micrometer to millimetre range, using light from a guide star. With these cophasing technique, the constraint of arranging the segments as a connex chain vanishes. Pupil densification no longer requires masking segments, which improves the limiting magnitude. However, it is unclear whether this allows comfortable observing, in the presence of flexure within the 100m mirror cell, which can proceed unchecked if a cloud momentarily crosses the aperture. Assessing the practical feasibility would require a comparison of the "blind lifetime" of mirror alignment with the recovery time following a cloud's crossing.

The non-connex segment arrays thus achievable in principle in the absence of edge sensors would relax constraints mentioned above for pupil densification, and make it more efficient.

The "dispersed speckle" method is a generalisation of the "dispersed fringes" measurement method used since Fizeau and Michelson, and computerized by Koechlin et al. for the GI2T interferometer. It measures piston errors among pairs of sub-apertures (Borkowski et al. 2005) by processing a series of images recorded simultaneously at different wavelengths. The recorded images are stacked (after correction of the dispersion effects) to build a cube called « dispersed image cube » (Figure 10).

A 3D Fourier transform of this cube gives an output cube in which there are « active » columns. Heights of "signal dots" appearing in active columns give piston measurements for the corresponding baseline.
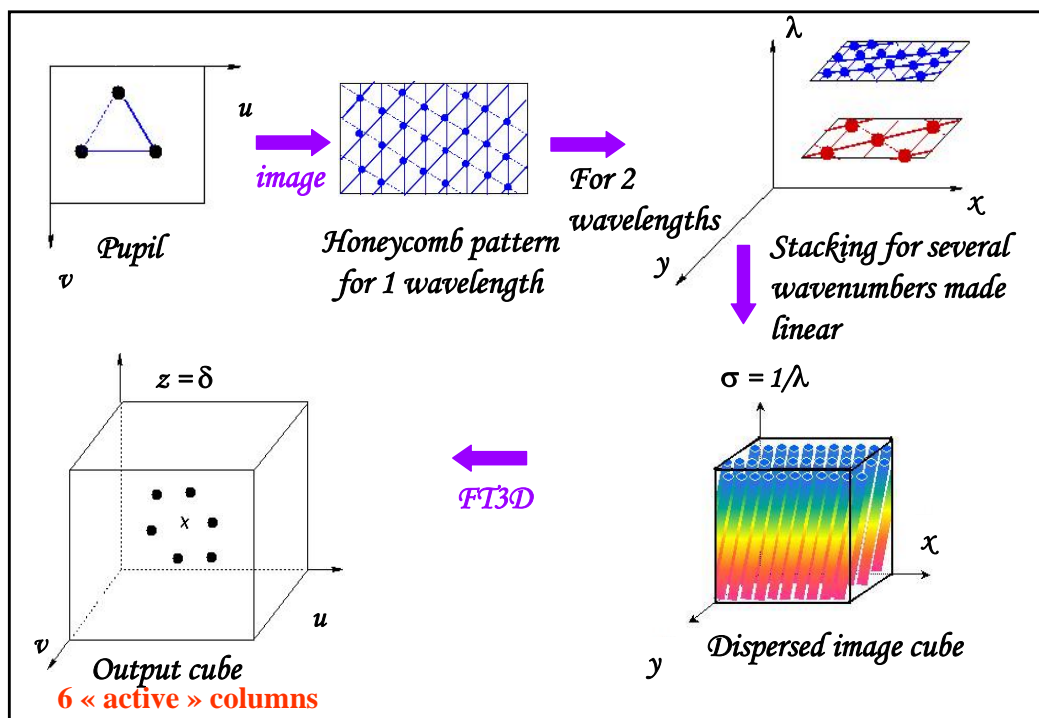

Figure 10: "Dispersed speckle" cophasing principle.

Positions of active columns match dot positions of the pupil autocorrelation. The number of active columns is *N(N-1)* ; with *N* the number of apertures.

Performances and limiting magnitudes of the "dispersed speckle" cophasing technique are summarised in the following table (1.6-m segments in a non-redundant array, J band, q_eff = 0.6; $\tau = 70\%$):

Observing mode	Cophasing precision *(rms)*	Required number of photons/cube	Limiting magnitude in J band
Minimum level for piston measurement	$\sim\lambda$	1600	14.6
Standard imaging	$\lambda/4$	3.2×10^4	11.3
High dynamic-range imaging	$\lambda/100$	3.2×10^5	8.8

10. Phased imaging with a partially filled aperture

The following step is coupling a segment phasing with an adaptive optics system to improve the sensitivity. The simulations shown assume phased apertures and thus indicate the direct imaging performance attainable with adaptive optics, in accordance with the discussions of hypertelescope properties published in the recent literature.

11. Coronagraphy : the ultimate step

Adaptive optics, if built to high specifications with many actuators, also allows coronagraphic imaging with a partially filled OWL in hypertelescope mode. This is of obvious interest for imaging the fainter exo-planets, but also cosmological objects such as active galactic nuclei and quasars.

If the output pupil is completely densified, coronagraphic techniques developed for mono-pupil telescope (cf. EPICS OWL instrument) are applicable for the hypertelescope mode of OWL. In the opposite case, the pupil should be reconfigured in a compact shape before the coronagraph as proposed for the VLTI hypertelescope mode (VIDA proposal). Most types of coronagraphic or apodizing optics are then usable in a way similar to that for a filled aperture.

The "extreme coronagraphy" techniques proposed for further attenuating the stellar residue after the coronagraphic occultor (Codona & Angel 2004, Labeyrie & Le Coroller 2004, Guyon 2004, Tolls et al. 2005, Nishikawa et al. 2005) are also applicable in the hypertelescope mode. For ground-based telescopes equipped with adaptive optics, their effectiveness will however be severely limited, in comparison with space telescopes, by the short life-time of the "seeing" residues. The photon noise in the briefly exposed residual speckles indeed affects the measurement of their modulus and phase, needed to null them interferometrically with a beam splitter or a dynamic hologram.

Detailed calculations are needed to estimate the exo-planet detection performance thus reachable. These calculations must include the effect of the parent star being partially resolved. As discussed by Martinache (thesis, 2005), the Lyot coronagraph, originally intended to observe the highly-resolved Sun, appears better in this respect than versions using a phase-mask.

12. Conclusion

The option of arranging a densified-pupil imaging mode during the few initial years of OWL observation can provide a moderate but useful gain of intensity and limiting magnitude. This is achievable with a small (typically 10-50cm), optical attachment near the focal plane, easily removable and having a comparatively low cost. Among the possible patterns of aperture filling, the concentring rings appear preferable, but more refined simulations can be envisaged. Non-isotropic pupil densification can be made with cylindrical lenses or mirrors.

We conclude that the pupil densification is justified with most imaging, spectro-imaging or coronagraphic instruments considered for initial observing with OWL. A specific instrument, in the form of a "hypertelescope camera", can be built.

Bibliography

Borkowski V. et al. 2005, A&A vol. 429, pp.747-753.

Codona J. & Angel R. 2004, Ap.J. 604, pp.L117-L120.

Guyon O. 2004, ApJ. 615, pp. 562-572.

Labeyrie A. & Le Coroller H. 2004, Proc. SPIE 5491, p.90.

Labeyrie A. et al. 1996, A&A Suppl. Series, v.118, pp.517-524.

Lardière O. et al. 2005, ESO Proc. on VLTI., in press.

Nishikawa J. et al. 2005, A&A 435, pp.3

Tolls V. et al. 2005, AAS Meeting 205, #171.04.